S38-34
160498
N93-27465

# A ROBUST QUASI-SIMULTANEOUS INTERACTION METHOD FOR A FULL POTENTIAL FLOW WITH A BOUNDARY LAYER WITH APPLICATION TO WING/BODY CONFIGURATIONS*)

A.J. van der Wees**) and J. van Muijden***)

National Aerospace Laboratory NLR
P.O. Box 90502; 1006 BM Amsterdam
The Netherlands
Tel: (020)5113113; Fax: (020)5113210

## Abstract

The MATRICS flow solver calculates the inviscid transonic potential flow about a wing/body semi-configuration. At present, work is in progress to extend MATRICS to take viscous effects into account through coupling with a boundary layer solver. This solver, MATRICS-V, is based on robust calculation methods for the boundary layer, the outer wing flow and their interaction. MATRICS-V is intended for (inverse) design purposes. The boundary layer and wake are based on an integral formulation of the unsteady first order boundary layer equations, the inviscid method is the existing MATRICS potential flow solver and the interaction algorithm is of the quasi-simultaneous type.

The paper gives a progress report on the coupled potential-flow boundary-layer method for transonic wing/body configurations.

## 1. Introduction

Computation methods for three-dimensional transonic potential flow are an important component in design systems for civil aircraft wing/body configurations. Accurate performance prediction under these conditions (e.g. lift-drag analysis) requires that the transonic potential flow solver is coupled with a boundary layer solver to account for the viscous effects on the wing pressure distribution in a sufficiently accurate way. For some years NLR has available its own developed system MATRICS (Multi-component Aircraft TRansonic Inviscid Computation System) for the calculation of the three-dimensional inviscid transonic potential flow about wing/body configurations (Ref. 1). The MATRICS-derivative MATRICS-V -now under development- will calculate the interaction of the inviscid potential outer flow and a viscous boundary layer on the wing of a transonic transport wing/body configuration. The ultimate objective of the development of MATRICS-V will be the embedding of this system in a wing design system, also currently under development at NLR.

This paper gives a progress report on the development of MATRICS-V. Firstly, a description will be given of the MATRICS three-dimensional transonic potential flow solver, being the starting point for the development of MATRICS-V. Secondly, the requirements for the development of the viscous-inviscid interaction solver will be formulated. Robustness of the interaction algorithm has been formulated as the main requirement. Next, the basic concepts of the viscous-inviscid interaction solver will be given. Subsequently, a short system overview will be given of the MATRICS-V flow solver, followed by an analysis of the boundary layer equation system and on the interaction law. Finally, some preliminary computational results will be presented.

## 2. Starting position for the development of MATRICS-V

The MATRICS-V viscous-inviscid interaction solver is a follow-up to the MATRICS three-dimensional inviscid transonic potential flow solver. This flow solver solves the full potential equation in strong conservation form on a grid of C-H or C-O topology. This grid is generated using the MATGRID grid generator (Tysell and Hedman, Ref. 2). The solver uses a fully conservative finite volume discretization and a multigrid solution method. The discretization scheme is second order accurate in the mesh size in subsonic parts of the flow, and first order accurate in supersonic parts of the flow. For the capture of supersonic/subsonic shock waves a Godunov-type shock operator is used. Options for fully-conservative as well as non-conservative shock-capture are available. Details on the MATRICS flow solver can be found in references 3, 4.
MATRICS provides data for a lift-drag-diving-moment analysis. Substantial research has been performed on the reliable prediction of drag by the MATRICS flow solver. Findings of this research have been reported in reference 5.

The development of MATRICS-V is partly based on experience at NLR with the modelling of two-dimensional strong viscous-inviscid interaction on airfoils (Refs. 6, 7).

## 3. Requirements

MATRICS-V is designed to calculate the influence of the wing boundary layer and wake on the inviscid potential outer flow about a given transport-type wing/body configuration from subsonic up to and including transonic cruise conditions. Laminar as well as turbulent boundary layers should be calculated, where the turbulent boundary layer is allowed to be mildly separated.
The MATRICS-V method should be robust; a guaranteed converged solution should be obtained for realistic flow conditions. The method should also be about ten times faster than a three-dimensional Reynolds-averaged Navier-Stokes solver, to enable wing design applications.

## 4. Basic concepts

The coupling of an inviscid outer flow with a viscous boundary layer flow will be done using an

---

*) This research has been performed under contract with the Netherlands Agency for Aerospace Programs (NIVR 01802N)
**) Research scientist, Num. Math. and Appl. Prog. Dep., Informatics Division
***) Research Scientist, Theoretical Aerodynamics Dep., Fluid Dynamics Division

integral method formulation of the boundary layer equations. With integral methods there is no explicit formulation of a turbulence model, but the system of equations is supplemented by suitable empirical closure relations. The integral method is reasonably easy to implement, because in the integral method the three-dimensional flow problem is formulated as a two-dimensional problem on the wing surface and the wake center-surface. This is a great advantage in code development.

Until a few years ago, the boundary layer equations have always been used in their steady form to compute a steady boundary layer flow. The main advantage of this formulation over an unsteady formulation has always been its lower computation time. However, using the boundary layer equations in their unsteady formulation, integrating them towards a steady solution, the boundary layer method is particularly well suited for vectorization and hence for implementation on todays supercomputers, see Van Dalsem and Steger (Ref. 8), Swafford and Whitfield (Ref. 9). An even more important advantage of using the unsteady boundary layer equations for solving steady boundary layer flow is the robustness of this approach. With the unsteady formulation a simple time-integration scheme will in any case produce an unsteady answer. With the steady formulation a space-marching scheme has to be used and the specification of initial data proves to be more difficult in a space-marching scheme than in a time-integration scheme. Also in case the steady boundary layer solution is non-unique or non-existent, the solution produced by an unsteady formulation is probably more useful, than the solution produced by a steady formulation.

Two candidate interaction algorithms have been considered, namely the semi-inverse and quasi-simultaneous algorithm. (The more sophisticated simultaneous algorithm is too expensive to implement in MATRICS because of the fully implicit relaxation algorithm employed in the existing inviscid potential outer flow solver). Experience by Ashill e.a. (Ref. 10), pp. 35, and Cebeci, Chen e.a. (Ref. 11) indicates that the semi-inverse algorithm lacks robustness in difficult flow cases. Therefore the quasi-simultaneous interaction algorithm is used, being the best available interaction algorithm that can be implemented in interaction with the inviscid potential outer flow solution algorithm.

In the inviscid potential outer flow solver the "blowing velocity approach" is used to account for the boundary layer effects on the inviscid outer flow, which means that a source strength is specified at the body surface and a jump in source strength at the wake. This approach is reasonably standard, while experience by Chen, Li e.a. (Ref. 12) reports that this approach is more reliable than the boundary layer displacement approach.

Experience by Chow (Ref. 13) indicates that it is mandatory to prescribe the pressure jump across the wake as a boundary condition to the outer inviscid flow. The latter jump influences the Kutta condition prescription in the outer inviscid flow, and this is essential in order to compute realistic lift values for the wing. The pressure jump across the boundary layer is computed as in Chow (Ref. 13) and Lock and Williams (Ref. 14).

## 5. Description of the calculation method

### 5.1 Inviscid method

The full potential equation

$$\frac{\partial}{\partial x^i}(\rho u^i) = 0, \tag{1}$$

$$u^i = u^i_\infty + \frac{\partial \varphi}{\partial x^i}, \tag{2}$$

$$q^2 = (u^1)^2 + (u^2)^2 + (u^3)^2, \tag{3}$$

$$\rho = \left\{1 + \frac{\gamma-1}{2} M_\infty^2 (1 - q^2)\right\}^{\frac{1}{\gamma-1}}, \tag{4}$$

is solved using a finite volume discretization formulated on a curvilinear coordinate system and a multigrid method employing ILU/SIP smoothing. At present only semi-configurations can be considered.

The boundary conditions are:

- on wetted surfaces $u_n = qS$; (5)
  for the inviscid flow solver, the source strength $S = 0$ on the body, else S is computed by the boundary layer solver;
- in the symmetry plane $u_n = 0$, (6)
- in the far-field, except downstream, $\varphi = 0$, (7)
- in the far-field downstream (Trefftz-plane)

$$\frac{\partial^2 \varphi}{(\partial \xi^1)^2} = 0, \tag{8}$$

  where $\xi^1$ is the chordwise (wrap-around) grid coordinate,
- across the prescribed vortex sheet

$$\begin{cases} [q] = q^+ - q^-, \\ [\rho u_n] = (\rho q S)^+ - (\rho q S)^- ; \end{cases} \tag{9}$$

  for the inviscid flow solver the jump across the wake, $(.)^+ - (.)^-$, is computed by the boundary layer solver,
- across the C-O topology branch cut that extends from the tip section to the far-field lateral boundary

$$[\varphi] = 0, \; [\rho u_n] = 0. \tag{10}$$

### 5.2 Viscous method

The steady first order boundary layer equations, describing conservation of mass and momentum in a general right-handed coordinate system, can be found in Myring (Ref. 15). Adding time-dependent terms and using first order integral thicknesses, the boundary layer equations can be integrated with respect to z (normal to the wing surface or wake centerline), using the momentum equation in z-direction to eliminate the pressure. Then the integral equations are obtained in the form

x-momentum:

$$\frac{1}{\bar{q}} \frac{\partial \delta_1}{\partial t} - \frac{\bar{u}}{\bar{q}^2} \frac{\partial \delta_p}{\partial t} + \left(\frac{1}{\bar{q}^2}(1-\bar{M}^2)\delta_1 + \frac{\bar{u}}{\bar{q}^3}\bar{M}^2\delta_\rho\right)\frac{\partial \bar{q}}{\partial t} +$$

$$\frac{1}{h_1}\frac{\partial\theta_{11}}{\partial x} + \theta_{11}\left\{\frac{2-\bar{M}^2}{h_1}\frac{1}{\bar{q}}\frac{\partial\bar{q}}{\partial x} + \frac{1}{J}\frac{\partial}{\partial x}\left(\frac{J}{h_1}\right) + k_1\right\} + \tag{11}$$

$$+ \frac{1}{h_2}\frac{\partial\theta_{12}}{\partial y} + \theta_{12}\left\{\frac{2-\bar{M}^2}{h_2}\frac{1}{\bar{q}}\frac{\partial\bar{q}}{\partial y} + \frac{1}{J}\frac{\partial}{\partial y}\left(\frac{J}{h_2}\right) + k_3\right\} +$$

$$\delta_1\left\{\frac{1}{h_1}\frac{1}{\bar{q}}\frac{\partial\bar{u}}{\partial x} + k_1\frac{\bar{u}}{\bar{q}}\right\} + \delta_2\left\{\frac{1}{h_2}\frac{1}{\bar{q}}\frac{\partial\bar{u}}{\partial y} + k_2\frac{\bar{v}}{\bar{q}} + k_3\frac{\bar{u}}{\bar{q}}\right\}$$

$$+ \theta_{22}k_2 = \frac{1}{2}C_{f_1};$$

y-momentum:

$$\frac{1}{\bar{q}}\frac{\partial\delta_2}{\partial t} - \frac{\bar{v}}{\bar{q}^2}\frac{\partial\delta_\rho}{\partial t} + \left\{\frac{1}{\bar{q}^2}(1-\bar{M}^2)\delta_2 + \frac{\bar{v}}{\bar{q}^3}\bar{M}^2\delta_\rho\right\}\frac{\partial\bar{q}}{\partial t} +$$

$$\frac{1}{h_1}\frac{\partial\theta_{21}}{\partial x} + \theta_{21}\left\{\frac{2-\bar{M}^2}{h_1}\frac{1}{\bar{q}}\frac{\partial\bar{q}}{\partial x} + \frac{1}{J}\frac{\partial}{\partial x}\left(\frac{J}{h_1}\right) + l_3\right\} + \tag{12}$$

$$+ \frac{1}{h_2}\frac{\partial\theta_{22}}{\partial y} + \theta_{22}\left\{\frac{2-\bar{M}^2}{h_2}\frac{1}{\bar{q}}\frac{\partial\bar{q}}{\partial y} + \frac{1}{J}\frac{\partial}{\partial y}\left(\frac{J}{h_2}\right) + l_2\right\} +$$

$$\delta_1\left\{\frac{1}{h_1}\frac{1}{\bar{q}}\frac{\partial\bar{v}}{\partial x} + l_1\frac{\bar{u}}{\bar{q}} + l_3\frac{\bar{v}}{\bar{q}}\right\} + \delta_2\left\{\frac{1}{h_2}\frac{1}{\bar{q}}\frac{\partial\bar{v}}{\partial y} + l_2\frac{\bar{v}}{\bar{q}}\right\}$$

$$+ \theta_{11}l_1 = \frac{1}{2}C_{f_2};$$

entrainment:

$$\frac{1}{\bar{\rho}\bar{q}J}\left\{\rho J\frac{\partial}{\partial t}(\delta-\delta_\rho) - J\frac{\bar{\rho}}{\bar{q}}\bar{M}^2(\delta-\delta_\rho)\frac{\partial\bar{q}}{\partial t} + \frac{\partial}{\partial x}\left[\frac{\rho J}{h_1}(\bar{u}\delta-\bar{q}\delta_1)\right] +\right.$$

$$\left.\frac{\partial}{\partial y}\left[\frac{\rho J}{h_2}(\bar{v}\delta-\bar{q}\delta_2)\right]\right\} = \frac{1}{\bar{q}}\left[\frac{\bar{u}}{h_1}\frac{\partial\delta}{\partial x} + \frac{\bar{v}}{h_2}\frac{\partial\delta}{\partial y} - \bar{w} + \frac{\partial\delta}{\delta t}\right] = C_E. \tag{13}$$

where q is the velocity, J is the Jacobien of the transformation from physical to computational space, and overbars denote boundary layer edge values. The density thickness $\delta_\rho$ is the integral of $(\bar{\rho}-\rho)/\bar{\rho}$ over the boundary layer.

In the latter equation (13) the instationary entrainment coefficient is an extension of the unsteady two-dimensional definition as used by Houwink (Ref. 16).

Subsequently an expression is needed for the calculation of the non-dimensional mass flux S through the surface of the wing and wake, representing the displacement effect of the boundary layer on the inviscid outer flow. Assuming an inviscid flow between the stream surface z = 0 and the displacement surface $\delta^*$, which is a stream surface for the inviscid flow, the following expression can be obtained from (13) by setting

$\delta = 0$:

$$S = \frac{1}{\bar{\rho}\bar{q}J}\left\{\rho J\frac{\partial\delta_\rho}{\partial\delta} - J\frac{\bar{\rho}}{\bar{q}}\bar{M}^2\delta_\rho\frac{\partial\bar{q}}{\partial t} + \frac{\partial}{\partial x}\left[\frac{\rho J}{h_1}\bar{q}\delta_1\right] + \frac{\partial}{\partial y}\left[\frac{\rho J}{h_2}\bar{q}\delta_2\right]\right\}; \tag{14}$$

this is equivalent to $S = \bar{w}/\bar{q}$, yielding the usual interpretation of S in steady inviscid flow.

In the used body-conforming non-orthogonal coordinate system the y-axis is in the spanwise direction of the wing, while the x-axis is in chordwise direction wrapping around the wing and the wake.

Next, a streamline coordinate system is adopted, in which the variables (now denoted with tildes) reduce to their familiar form, see Myring (Ref. 15). Transformation to and from the streamline coordinate system is done whenever necessary. Thus it is possible to derive equations using the well-known integral parameters in streamline coordinates and in the curvilinear system.

The equations (11) to (14) are thus written in the basic variables $\bar{\theta}_{11}$, $\bar{H}$, $\bar{q}$ and C, where the cross-flow parameter C is defined as

$$C = \frac{\mathrm{sign}(\beta_w)\sqrt{-\bar{\theta}_{22}}}{\bar{\delta}_1} \tag{15}$$

Reduction of the number of unknowns to the four basic variables is established by prescribing a set of turbulent velocity profiles in the streamline coordinate system, while the density thickness $\delta_\rho$ is eliminated using the Crocco relation, prescribing a parabolic distribution between velocity and temperature (Ref. 17). For the time being no velocity profiles are used, but proven closure relations taken from accepted two-dimensional methods for attached as well as separated flow (Ref. 16, 18, 19) have been implemented in a first version of the code. In a next version, more physical closure relations and velocity profile families will be used.

Initial conditions for the turbulent boundary layer calculation are generated by the BOLA-2D solver (Ref. 20), which calculates the laminar quasi-two-dimensional flow in the leading edge region of the wing.

Boundary conditions are set at the wing root, where derivatives in spanwise direction are assumed to be zero, and the wing tip, where zero lateral derivatives in local sweep direction are prescribed, see Cross (Ref. 21). Far downstream, a zero gradient condition in chordwise direction is specified for all quantities.

The system of equations (11) to (13) is solved in combination with an interaction law (to be discussed in the next section). The complete set of equations can be written symbolically as

$$\frac{E}{\bar{q}}u_t + Au_x + Bu_y + Du = f, \qquad (16)$$

where $u = [\bar{\theta}_{11}, \bar{H}, \bar{q}, C]$.

The system (16) appears to be hyperbolic in practice. Discretization is done according to the directions of the characteristics in (x,t) and (y,t)-space, using a matrix-split procedure (Ref. 22). Thus equation (16) is discretized as

$$\frac{E}{\bar{q}}u_t + A^+\vec{\partial}_x u + A^-\vec{\partial}_x u + B^+\vec{\partial}_y u + B^-\vec{\partial}_y u + Du = f. \qquad (17)$$

In smooth parts of the flow second order accurate differencing will be obtained using a scheme as for example in Spekreijse (Ref. 23).
The system of equations (17) is solved using the fully implicit backward Euler time-integration scheme proposed by Steger and Warming (Ref. 24) and Yee (Ref. 25).

## 5.3 Interaction law

In order to avoid a breakdown of the boundary layer formulation in separated flow regions an extra equation is needed which modifies the inviscid flow boundary layer edge velocity $\bar{q}$. Usually a highly linearized form of the inviscid outer potential flow is taken, for example the two-dimensional Hilbert-integral formulation as used by Veldman (Ref. 26). An even more simplified form is given by Williams (Ref. 27). In this paper the latter form is slightly modified, but still derived from the linearized potential equation. This will be discussed in more detail in section 6.2. In its simplest form the interaction law can be written as

$$\frac{\partial \bar{q}}{\partial s} - \frac{\bar{q}\pi}{\beta\Delta x}S = \left(\frac{\partial \bar{q}}{\partial s}\right)^k - \frac{\bar{q}^k\pi}{\beta^k\Delta x}S^k. \qquad (18)$$

Time-dependent terms are obtained from the instationary form of S (equation (4)), paying special attention to the limiting case for $\bar{M} \to 0$.
Two remarks are made:

1. Equation (18) is written along streamlines, which implies that the streamline directions are known from the inviscid flow solver and are kept fixed during a viscous calculation.
2. Equation (18) is a law in correction form, indicating that it will not influence the converged solution. In this way the interaction law can be shown to be essential to avoid breakdown of the boundary layer formulation, but once convergence is obtained it does not affect the final solution.

## 5.4 Viscous-inviscid interaction algorithm

The leading edge part of the boundary layer will be calculated in direct mode using the program BOLA-2D (Ref. 20). This presupposes that the flow does not separate in this part of the boundary layer. The inviscid flow computation in this part is done in direct mode with a source strength S specified on the wing. Further downstream, a quasi-simultaneous interaction algorithm is used. In this formulation the inviscid flow calculation is done in direct mode with a prescribed source strength S on the wing and the wake and a prescribed velocity jump across the wake. The viscous calculation is done in quasi-simultaneous mode with a prescribed inviscid wall velocity, which has been corrected for boundary layer curvature effects. Thus the boundary layer is computed effectively with a prescribed edge velocity instead of the inviscid wall velocity. Cebeci, Clark e.a. (Ref. 28) have shown that such an approach avoids the initiation of undesirable pressure fluctuations in the trailing-edge region at reasonably large angles of attack. The boundary layer computation computes a new source strength S and velocity jump $\Delta q$, which are used as the subsequent input for the interactive calculations.

# 6. Analysis of the system of equations

## 6.1 Analysis of boundary layer equation system

To analyze the properties of the boundary layer equations formulated in chapter 5 (Eqs. (1), (2), (3), (18)) we assume the following simplifying conditions:

- orthonormal coordinate system, i.e. $h_1=h_2=1$, $g=0$; $k_1=k_2=k_3=0$; $l_1=l_2=l_3=0$;
- outer streamline aligned with the x-axis, i.e. $\bar{u}/\bar{q}=1$, $\bar{v}/\bar{q}=0$;
- closure conditions as in Cousteix and Houdeville (Ref. 20), i.e.

$$\bar{\theta}_{12} = C(\bar{\delta}_1-\bar{\theta}_{11}),\ \bar{\theta}_{21} = -C\bar{\theta}_{11},$$

$$\bar{\theta}_{22} = -C^2(\bar{\delta}_1-\bar{\theta}_{11}),\ \bar{\delta}_2 = -C\bar{\delta}_1. \qquad (19)$$

With $H=\bar{\delta}_1/\bar{\theta}_{11}$ and $H_1=(\delta-\bar{\delta}_1)/\bar{\theta}_{11}$ we obtain an equation system

$$\frac{E}{\bar{q}}u_t + Au_x + Bu_y = f,\ u = [\ln\bar{\theta}_{11}, \bar{H}, \ln\bar{q}, \ln C],$$

where

$$E = \begin{bmatrix} H-\bar{H}(\bar{H}+1)\delta_r & 1 & -H(\bar{H}^2-1)+\bar{H}^2\delta_r(\bar{H}+1) & 0 \\ H+H_1-\delta_r(\bar{H}+1) & H_1'+1 & -\bar{H}^2(H+H_1-\delta_r(\bar{H}+1) & 0 \\ -K_1(\delta_r+\epsilon)(\bar{H}+1) & -K_1(\epsilon+\delta_r) & -(\bar{H}+1)(2\epsilon K_1+\bar{H}_q\delta_r K_1-\bar{H}^2\delta_r K_d) & 0 \\ H & \delta_r+1 & H(1-\bar{H}^2)+\bar{H}_q\delta_r(\bar{H}+1) & H \end{bmatrix}, \qquad (20)$$

$$A = \begin{bmatrix} 1 & 0 & H+2-\bar{H}^2 & 0 \\ H_1 & H_1' & H_1(1-\bar{H}^2) & 0 \\ -HK_1 & -K_1(\delta_r+1) & K_d-K_1\bar{H}_q\delta_r(\bar{H}+1) & 0 \\ 1 & 0 & 2-\bar{H}^2 & 1 \end{bmatrix}, \qquad (21)$$

$$B = \begin{bmatrix} H-1 & \delta_r+1 & (1-\bar{H}^2)H+(\bar{H}+1)\bar{H}_q\delta_r+\bar{H}^2-2 & H-1 \\ H & \delta_r+1 & (1-\bar{H}^2)H+(\bar{H}+1)\bar{H}_q\delta_r & H \\ 0 & 0 & 0 & 0 \\ C(H-1) & C(\delta_r+1) & C((H-1)(2-\bar{H}^2)+(\bar{H}+1)\bar{H}_q\delta_r) & 2C(H-1) \end{bmatrix}; \qquad (22)$$

the parameter $\epsilon \neq 0$ at $\bar{M}=0$ and

$$\delta_r = \frac{\gamma-1}{2} r\bar{M}^2, \tag{23a}$$

$$\bar{M}_q = 2 + (\gamma-1)\,\bar{M}^2, \tag{23b}$$

$$H = (\bar{H}+1)(1+\bar{\delta}_r) - 1, \tag{23c}$$

$$H_1' = dH_1/dH. \tag{23d}$$

Setting $K_d=1$ and $K_i=\pi/(\beta\Delta x)$ in the third row of eqs. (20)..(22) reproduces eq. (18).

Following Myring, reference 16, the characteristics of an equation

$$Eu_t + Au_x + f = 0,\ u = [u_1 \ldots u_n]$$

can be obtained from

$$\det(E-\lambda A) = 0,\ \lambda = \frac{dt}{dx}. \tag{24}$$

We first consider the quasi two-dimensional flow case ($\partial/\partial y=0$) where no interaction law is used, i.e. $K_i=0$, $K_d=1$. This way we find the following expressions for the characteristic directions $\lambda$:

$$\lambda = H, \tag{25a}$$

$$\lambda = \bar{M}_q\delta_r(\bar{H}+1), \tag{25b}$$

$$-H_1'\lambda^2 + ((H+1)H_1' - H_1 + 1 - (\bar{H}+1)\delta_r H_1')\,\lambda +$$

$$- HH_1' + H_1 + (\bar{H}+1)\delta_r H_1' = 0. \tag{25c}$$

For realistic $H_1(H)$-functions, viz. with $H_1'-H_1/\bar{H}$ the roots of the latter quadratic equation are real. Consequently, the equation system is fully hyperbolic. If $H_1'<0$ the values for $\lambda$ are greater than zero. At separation, that is at $H_1'=0$, in the minimum of the $H_1(\bar{H})$ curve, one eigenvalue $\lambda$ passes through zero, which means that the characteristic direction changes from upwind to downwind there. Consequently, the equation system models the corresponding physical behaviour.

We continue the analysis for the quasi two-dimensional case ($\partial/\partial y=0$), but now for the case where an interaction law is used to solve for $\ln\bar{q}$, i.e. $K_i\neq 0$, $K_d=1$. In case $K_i=1$, $\bar{M}^2=0$ and $\epsilon=0$ we find the following expressions for $\lambda$:

$$\lambda = 0, \tag{26a}$$

$$\lambda = H, \tag{26b}$$

$$((H+1)^2H_1' - (H+1)H_1)\,\lambda^2 + (-H_1'(2H+1)(H+1) +$$

$$+ H_1(2H+3) - 1)\,\lambda + (H+1)(HH_1' - H_1) = 0. \tag{26c}$$

For realistic $H_1(\bar{H})$-functions, namely with $(H+1)H_1'-H_1<0$ and $HH_1'-H_1<0$ three values for $\lambda$ are positive, one is negative. For small $\epsilon<0$ it can be shown that all values for $\lambda$ are positive for all H, so that now all characteristics originate from the upwind direction.

For the case $\partial/\partial y\neq 0$ we find the following characteristic directions in the x,y-plane ($\lambda=dy/dx$):

- No interaction law ($K_i=0$, $K_d=1$):

$$\lambda = 0, \tag{27a}$$

$$\lambda = H-1, \tag{27b}$$

$$H_1'\lambda^2 + ((H-1)H_1' - H_1(1+\delta_r) + 1 + \delta_r)\,\lambda +$$

$$+ 1 + \delta_r = 0; \tag{27c}$$

as in the x,t-plane a characteristic direction changes from upwind to downwind at separation (i.e. at $H_1'=0$).

- With interaction law ($K_i\neq 0$, $K_d=1$) in case $K_i=1$, $\bar{M}^2=0$, $\epsilon=0$:

$$\lambda = 0, \tag{28a}$$

$$(-(H+1)^2H_1' + (H+1)H_1)\lambda^3 + ((2H^3+H^2-2H-2)H_1' +$$

$$+(-2H^2+1)H_1 + H^2 + H + 1)\lambda^2 +$$

$$+((H^2-1)H_1' + H^2 + H + 2)\lambda + 1 = 0; \tag{28b}$$

two positive and one negative value for $\lambda$ are found in case of realistic $H_1(H)$-functions.

The characteristics in the x,t-plane for the more general case with an interaction law ($K_i\neq 0$) and without the additional settings $K_i=1$, $\bar{M}^2=0$ and $\epsilon=0$ can only be analyzed numerically. We find the following expressions for the characteristic directions:

$$\lambda = H, \tag{29a}$$

$$a_3\lambda^3 + a_2\lambda^2 + a_1\lambda + a_0 = 0, \tag{29b}$$

where $a_3 = \det A$ and $a_0 = \det E$.
A well-defined interaction law has the property that $a_3\neq 0$ for all $\bar{H}$. This gives the following relation between $K_i$ and $K_d$:

$$K_i > \frac{-H_1'}{(HH_1'-H_1)(H+1) - \delta_r\bar{M}_q H_1'(\bar{H}+1) + HH_1'(1-\bar{M}^2) - H_1\delta_r(H+1)}\,K_d, \tag{30}$$

if $H_1'<0$ the value $K_i=0$ may be chosen (direct mode). If $H_1'<0$ the value $K_i=0.01K_d$ is suitable for all $\bar{M}^2$ and all $\bar{H}$, in the sense that numerical computation of $\lambda$ indicates that then for $0<\bar{M}^2<1.7$ all values for $\lambda$ are real and positive, while in some rare cases complex values are found with a positive real part. The boundary layer equation system (and interaction law) have consequently favourable properties for use in the transonic flow regime at cruise conditions. Because all characteristic directions generally originate from upstream, initial conditions for $\bar{\theta}_{11}$, $\bar{H}$, $\bar{q}$ and C have to be

specified upstream, while downstream no initial conditions need be specified.

### 6.2 Properties of interaction law

Following Lock and Williams (Ref. 14), we consider a source strength S approximately normal to the surface, a velocity q approximately parallel to the surface, and define a perturbation potential $\phi$ as

$$\frac{\Delta q}{q} = \phi_s, \quad \Delta S = \phi_z. \tag{31}$$

The outer potential flow can be described by the linearized perturbation potential equation

$$(1-M^2)\,\phi_{ss} + \phi_{zz} = 0,$$

$$\text{with } \phi_z = \Delta S \text{ at } z = 0. \tag{32}$$

In the context of the definition of an interaction law we will interprete $\Delta q/q$ and $\Delta S$ as corrections with respect to a starting solution, i.e.

$$\frac{\Delta q}{q} = \frac{q-q^k}{q}, \quad \Delta S = S-S^k, \tag{33}$$

where $q^k$ is given by the preceeding outer flow computation and $S^k$ by the preceeding viscous flow calculation. A solution to (32) in subsonic flow in Fourier space is given by

$$\phi = Ce^{i\nu s}e^{-\beta\nu z}, \quad \beta = \sqrt{|1-M^2|}. \tag{34}$$

Algebraic manipulation of (31), (32) and (34), using the derivative of $\Delta q/q$ with respect to s in order to obtain non-imaginary quantities, then leads to a law in Fourier space of the form

$$\beta\left(\frac{1}{q}\frac{\partial q}{\partial s} - \frac{1}{q^k}\frac{\partial q^k}{\partial s}\right) = \nu(S-S^k). \tag{35}$$

In physical space we may consider (35) as the leading term in an integral form of an interaction law and use it in this simplified form.
In supersonic flow only the right-running wave is considered,

$$\phi = Ce^{i\nu s}e^{-i\beta\nu z}. \tag{36}$$

Manipulation now yields a non-imaginary interaction law of the form

$$\beta\,\frac{q-q^k}{q} = -(S-S^k). \tag{37}$$

Considering eq. (37) as the leading term of an integral form of an interaction in physical space, we now have a form of interaction law that couples S to q instead of $\partial q/\partial s$, which cannot be incorporated in the system of boundary layer equations in a simple way. The subsonic law (35) appears however to produce useful results both in subsonic and supersonic flow, which is mainly due to the fact that strong interaction occurs in subsonic parts of the flow (at supersonic-subsonic shock waves and at trailing edges). This relaxes the need for an explicit supersonic law, also considering the findings described in section 5.1. We will therefore use eq. (35) both in supersonic and subsonic flow.

Parameters are now introduced for the direct and inverse parts of eq. (35):

$$K_d\beta\left(\frac{1}{q}\frac{\partial q}{\partial S} - \frac{1}{q^k}\frac{\partial q^k}{\partial S}\right) = \nu K_i(S-S^k). \tag{38}$$

The parameters $K_i$ and $K_d$ can be used to perform direct, inverse and quasi-simultaneous computations as follows:

| | | |
|---|---|---|
| direct | : $K_i = 0$, $K_d = 1$, | (39a) |
| inverse | : $K_i = 1$, $K_d = 0$, | (39b) |
| quasi-simultaneous | : $K_i > 0$, $K_d = 1$. | (39c) |

With quasi-simultaneous computations, inspection of equation (3.8) shows that the inviscid outer flow solution is modified locally at places where S differs much from the previous solution $S^k$. In the first few iterations between inner and outer solver this will lead to non-physical velocity distributions in the boundary layer, especially at the wake where a velocity difference will occur between upper and lower side for lifting cases, showing the deficiency of not modelling the circulation in the interaction law. The inviscid flow solver will therefore have to compute this circulation effect on its own.

Considering the two-dimensional steady form of S and using the property of mass conservation along streamlines in the outer flow, we will use in eq. (38):

$$S = \frac{\partial \delta^*}{\partial S}. \tag{40}$$

It can now be observed that with $K_i>0$ and $K_d>0$ in equation (38) $\partial q/\partial s$ has a positive correlation with $\partial\delta^*/\partial s$, which is a desired property in subsonic flow.

## 7. Preliminary computational results

The MATRICS inviscid flow solver has been tested extensively and appears to be a robust method (Ref. 3, 4). In this section attention will be given to the boundary layer solver with interaction law and its robustness. Finally a fully converged solution of the whole viscous-inviscid interaction computation will be shown.
Starting with an inviscid velocity distribution provided by the MATRICS outer solver, some calculations have been made to obtain a converged boundary layer solution only.
Initial values for the boundary layer parameters were obtained from a two-dimensional flat plate solution. These calculations, without any interaction with the inviscid outer solver, show the changes made by the interaction law.

The first case is a NACA-0012 straight wing at a Mach number of 0.70, zero angle of attack and Reynolds number of 9 million. Only the root section of the wing will be shown, because this section is a symmetry plane with a two-dimensional flow by definition, and therefore allows comparison with two-dimensional methods. In figure 1a the inviscid velocity distribution at the root section is given. It can be shown that the trailing edge stagnation behaviour causes a severe boundary layer growth, leading to separation if no interaction law is used to adapt the velocity distribution. Figures 1b, c, d show the resulting velocity, momentum thickness and shape factor H at Reynolds number of 9 million,

calculated with interaction factor $K_i$=0.05. The resulting velocity distribution shows smaller decelerating velocity gradients and a less severe stagnation behaviour at the trailing edge. In order to obtain a physically relevant viscous solution, the outflow, computed from this very first boundary layer solution, can be added to the full inviscid flow solver for an adjustment of the inviscid flow to the boundary layer effect. A fully converged viscous-inviscid solution requires a number of such interations between the inviscid flow solver and the boundary layer/interaction law computation.

The second case is the same straight wing at Mach number of 0.799, angle of attack of 2.26 degrees, and a Reynolds number of 9 million. The inviscid velocity distribution at the root section (Fig. 2a) will certainly cause separation on the upper side of the wing. Starting from a very simple flat plate momentum thickness distribution, large changes must be expected in the velocity gradients. In this case, the resulting momemtum thickness at the trailing edge is much below the viscous-inviscid converged value, due to the changes in velocity distribution, while the shape factor $\bar{H}$ is only showing separation just behind the shock wave (Fig. 2b, c, d). In the viscous-inviscid converged solution separation will probably occur from shock to trailing edge (Ref. 29). The non-physical velocity jump across the wake (Fig. 2b) is due to the asymmetry of the computed flow and the simplicity of the interaction law. In the iterative process between the full inviscid flow solver and the boundary layer/interaction law, however, the errors due to the simplicity of the interaction law should disappear, resulting in a converged solution and an inactive interaction law.

Figures 3a and 3b show the convergence histories of the residuals of the x-momentum equation, entrainment equation and interaction law of the boundary layer equation system for the testcases presented in figures 1 and 2. Using the same computational parameters, both convergence histories show a robust convergence, which means that a converged solution can be computed even when the inviscid flow velocity distribution and the starting solution for the boundary layer flow do not at all fit together.

At the time of writing of the paper, work on the interaction algorithm was making good progress. A first fully converged interacting solution has been obtained for the attached flow around the NACA-0012 wing at a Mach number of 0.70, angle of attack of 1.49 degrees, and a Reynolds number of 9 million. The boundary layer is computed with an increasing part of the inviscid flow velocity in the first few iterations, while underrelaxation is applied to the source strength that is used as input to the outer solver. No boundary layer curvature effects have yet been accounted for. Using this procedure the inner and outer flow are smoothly adapted to each other.
In figure 4 the initial inviscid velocity distribution (viz. without a boundary layer effect) is shown, together with the final viscous velocity distribution and the corresponding boundary layer variables. The difference between the inviscid and viscous velocity is small, except at the trailing edge, where the boundary layer displacement effect is appreciable. This testcase has been calculated with thirteen viscous-inviscid iterations in order to obtain a converged lift value. The convergence history is shown in figure 5a. Finally, in figure 5b the convergence history of the residuals in the MATRICS outer flow solver are given as a function of the number of smoothings. A reduction in both maximum and mean value residual of 2.5 orders of magnitude has been obtained, which is promising for further development of the interaction algorithm.

## 8. References


1. Vooren, J. van der, Wees, A.J. van der, Meelker, J.H., MATRICS, Transonic Potential Flow Calculations About Transport Aircraft. In: AGARD Conf. Proc. No. 412, 1986
2. Tysell, L.G., Hedman, S.G., Towards a General Three-Dimensional Grid Generation System. ICAS-88-4.7.4, 1988
3. Wees, A.J. van der, A Nonlinear Multigrid Method for Three-Dimensional Transonic Potential Flow. Ph. D. thesis, University of Technology Delft, The Netherlands, 1988
4. Wees, A.J. van der, Impact of Multigrid Smoothing Analysis on Three-Dimensional Potential Flow Calculations. In: Mandel, J., e.a. (eds.), Proc. 4th Copper Mountain Conf. on Multigrid Methods, SIAM Proceedings, ISBN 0-89871-248-3, 1989
5. Vooren, J. van der, Wees, A.J. van der, Inviscid Drag Prediction for Transonic Transport Wings Using a Full-Potential Method, AIAA-90-0576, January 1990 (accepted for publication in AIAA Journal)
6. Veldman, A.E.P., Lindhout, J.P.F., Boer, E. de, Somers, M.A.M., VISTRAFS, a Simulation Method for Strongly-Interacting Viscous Transonic Flow. NLR MP 88061 U, 1988
7. Houwink, R., Veldman, A.E.P., Steady and Unsteady Separated Flow Computations for Transonic Airfoils. NLR MP 84028 U, 1984
8. Dalsem, William R. van, Steger, Joseph L., Efficient Simulation of Separated Three-Dimensional Viscous Flows using the Boundary-Layer Equations, AIAA Journal Vol. 25, No. 3, 1987
9. Swafford, T.W., Whitfield, D.L., Time-Dependent Solution of Three-Dimensional Compressible Turbulent Integral Boundary-Layer Equations, AIAA Journal Vol. 23, No. 7, July 1985
10. Ashill, P.R., Wood, R.F., Weeks, D.J., An Improved, Semi-Inverse Version of the Viscous Garabedian and Korn Method (VGK), RAE Techn. Report 87002, 1987
11. Cebeci, T., Chen, L.T., Chang, K.C., Peavey, C.C., An Interactive Scheme for Three-Dimensional Transonic Flows, Proc. 3rd Symp. on Num. and Phys. Aspects of Aerodyn. Flows, pp. 11-39 - 11-49, 1985
12. Chen, L.T., Li, S, Chen, H., Calculation of Transonic Airfoil Flows by Interaction of Euler and Boundary-Layer Equations, AIAA-87-0521, 1987
13. Chow, R., Solution of Viscous Transonic Flow over Wings, Computers & Fluids Vol. 13, No. 3, pp. 285-317, 1985
14. Lock, R.C., Williams, B.R., Viscous-Inviscid Interactions in External Aerodynamics, Prog. Aerospace Sci. Vol. 24, pp. 51-171, 1987
15. Myring, D.F., An Integral Prediction Method for Threedimensional Turbulent Boundary Layers in Incompressible Flow, RAE Techn. Report 70147, 1970
16. Houwink, R., Veldman, A.E.P., Steady and Unsteady Separated Flow Computations for

Transonic Airfoils, AIAA-84-1618, 1984
17. Cebeci, T., Smith, A.M.O., Analysis of Turbulent Boundary Layers. Academic Press, 1974
18. Green, J.E., Weeks, D.G., Brooman, J.W.F., Prediction of Turbulent Boundary Layers and Wakes in Compressible Flow by a Lag-Entrainment Method, ARC R&M 3791, 1973
19. Cousteix, J., Houdeville, R., Singularities in Three-Dimensional Turbulent Boundary-Layer Calculations and Separation Phenomena, AIAA Journal, Vol. 19, No. 8, pp. 976-985, 1981
20. Bruin, A.C. de, Boer, E. de, Users Guide of BOLA-2D, the NLR-method for the Calculation of (Quasi) Two-dimensional Boundary Layers, NLR memorandum AI-82-014 U, 1982
21. Cross, A.G.T., Calculation of Compressible Three-Dimensional Turbulent Boundary layers with Particular Reference to Wings and Bodies, YAD Note 3379, November 1979
22. Hartwich, P.M., Split Coefficient Matrix (SCM) Method with Floating Shock Fitting for Transonic Airfoils. Proc. Int. Conf. on Num. Meth. in Fluid dynamics, Oxford, July 1990
23. Spekreijse, S., Multigrid Solution of Monotone Second-order Discretizations of Hyperbolic Conservation Laws, Math. Comp. Vol. 49, No. 179, pp. 135-155, July 1987
24. Steger, J.L., Warming, R.F., Flux Vector Splitting of the Inviscid Gasdynamic Equations With Application to Finite Difference Methods, NASA-TM-78605, 1979
25. Yee, H.C., Upwind and Symmetric Shock-Capturing Schemes, NASA-TM-89464, 1987
26. Veldman, A.E.P., A new Quasi-Simultaneous Method to Calculate Interacting Boundary Layers. AIAA J, Vol. 19, pp. 79-85, 1981
27. Williams, B.R., Coupling Procedures for Viscous-Inviscid Interaction in External Aerodynamics. In: Proc. 4th Symp. on Num. and Phys. Aspects of Aerodyn. Flows, Long Beach, CA, January 1989
28. Cebeci, T., Clark, R.W., Chang, K.C., Halsey, N.D., Lee, K., Airfoils with Separation and the Resulting Wakes, Proc. 3rd Symp. on Num. and Phys. Aspects of Aerodyn. Flows, pp. 2-13 - 2-26, 1985
29. Holst, T.L., Viscous Transonic Airfoil Workshop Compendium of Results. AIAA-87-1460, 1987

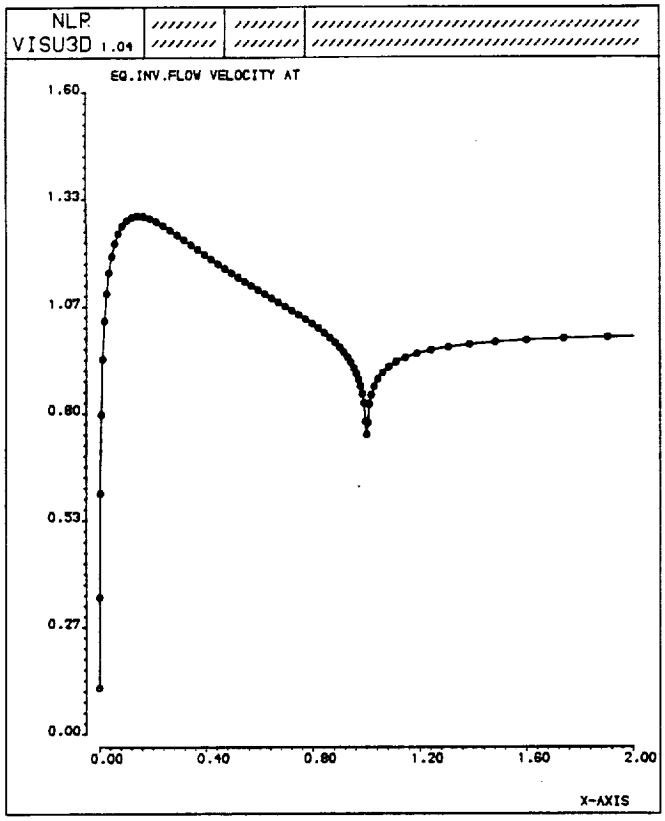


a) Inviscid flow velocity distribution

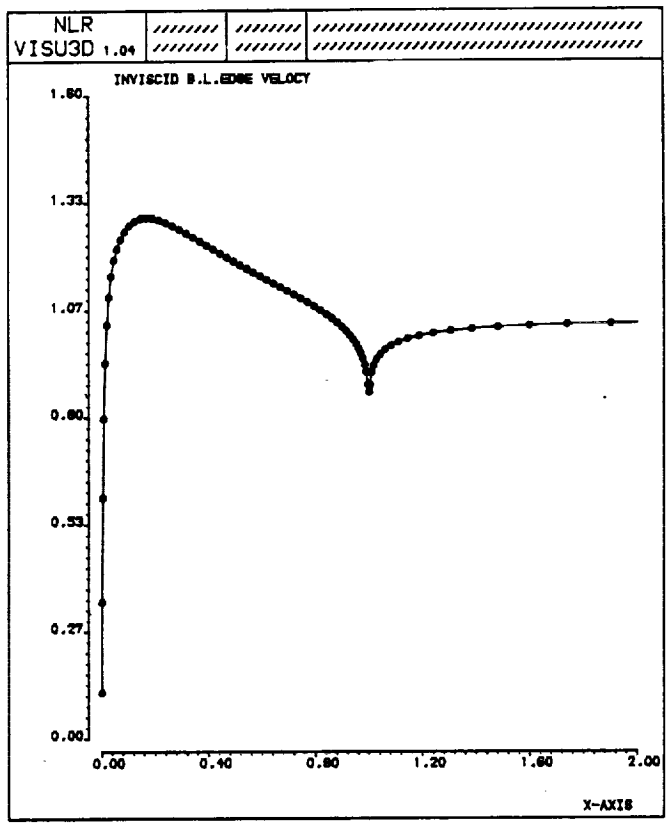


b) Boundary layer inviscid edge velocity

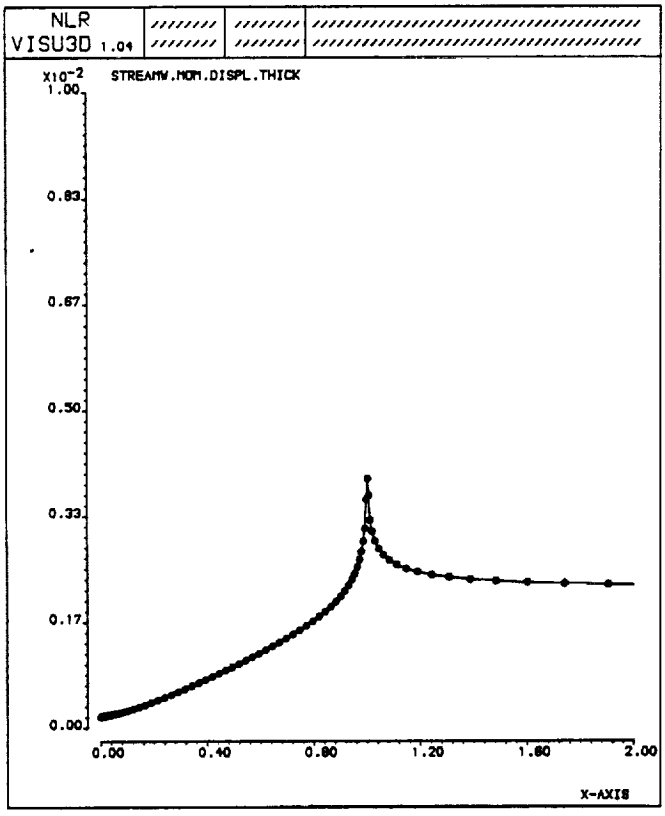


c) Boundary layer streamwise momentum thickness

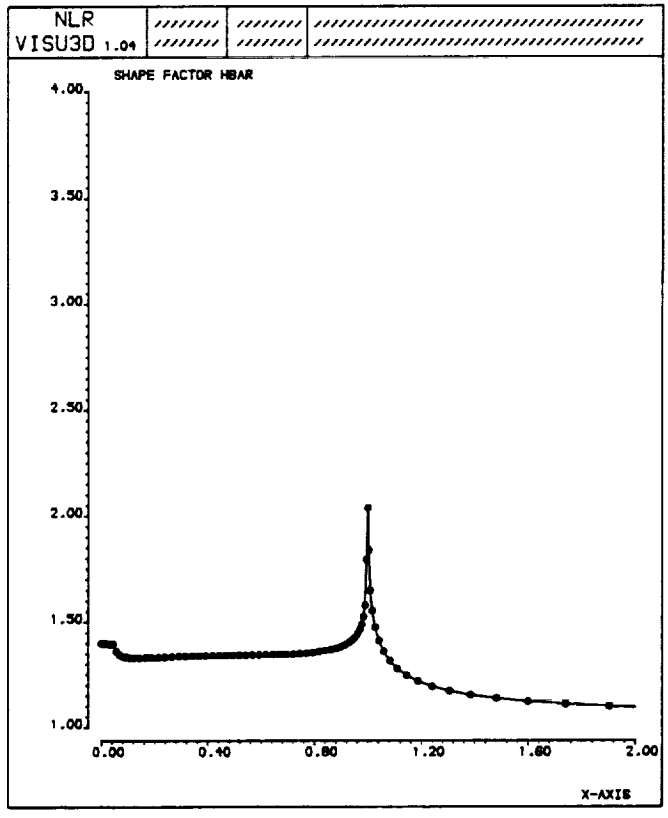


d) Boundary layer shape factor $\overline{H}$

Fig. 1 Boundary layer results for root section of a NACA-0012 straight wing at $M_\infty = 0.70$, $\alpha = 0$, $Re = 9 * 10^6$

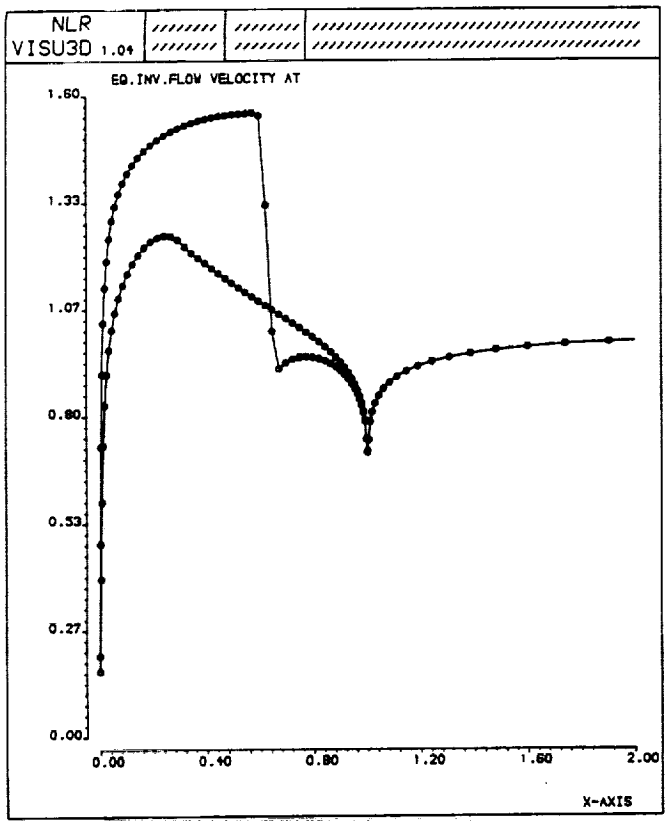


a) Inviscid flow velocity distribution

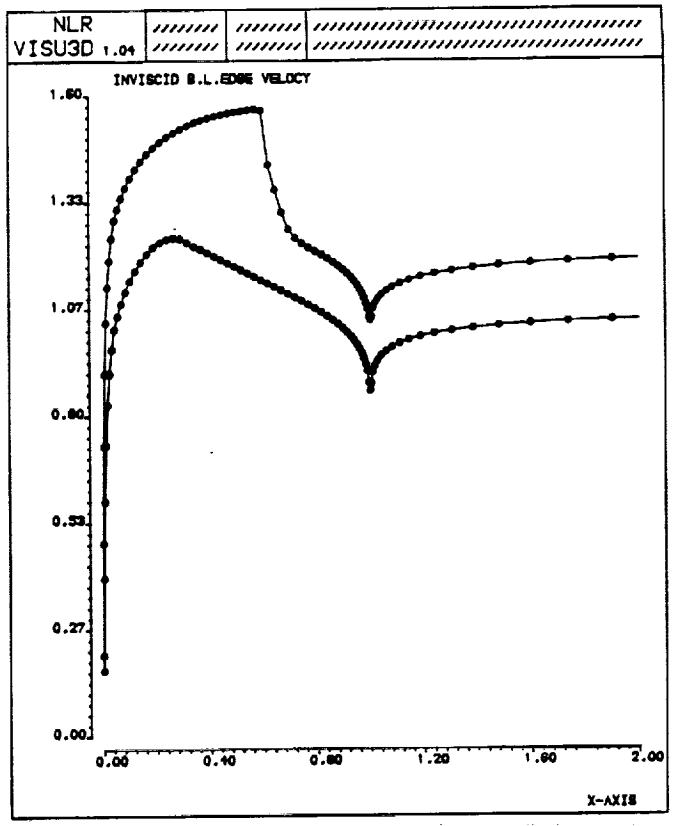


b) Boundary layer inviscid edge velocity

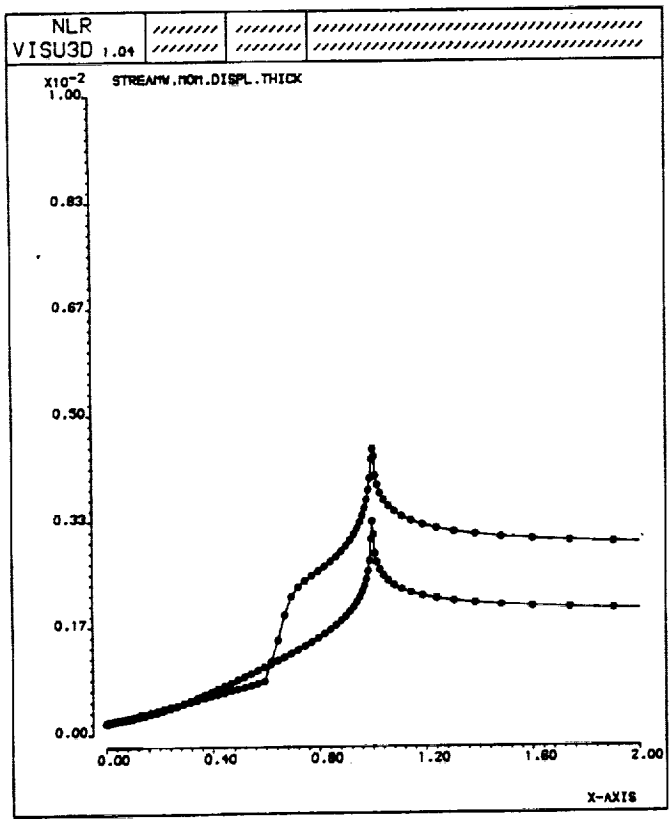


c) Boundary layer streamwise momentum thickness

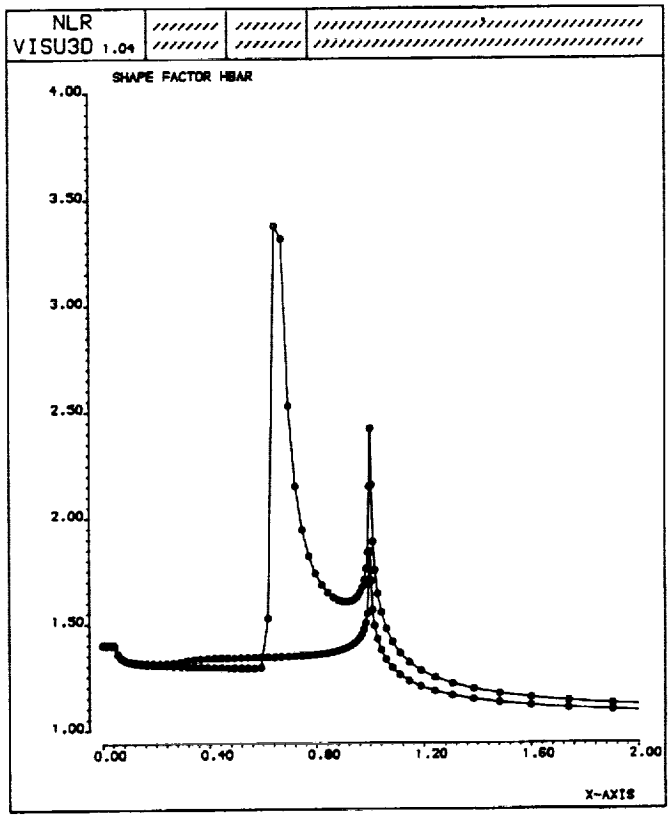


d) Boundary layer shape factor $\overline{H}$

Fig. 2 Boundary layer results for root section of a NACA-0012 straight wing at $M_\infty = 0.799$, $\alpha = 2.26$, $Re = 9 * 10^6$

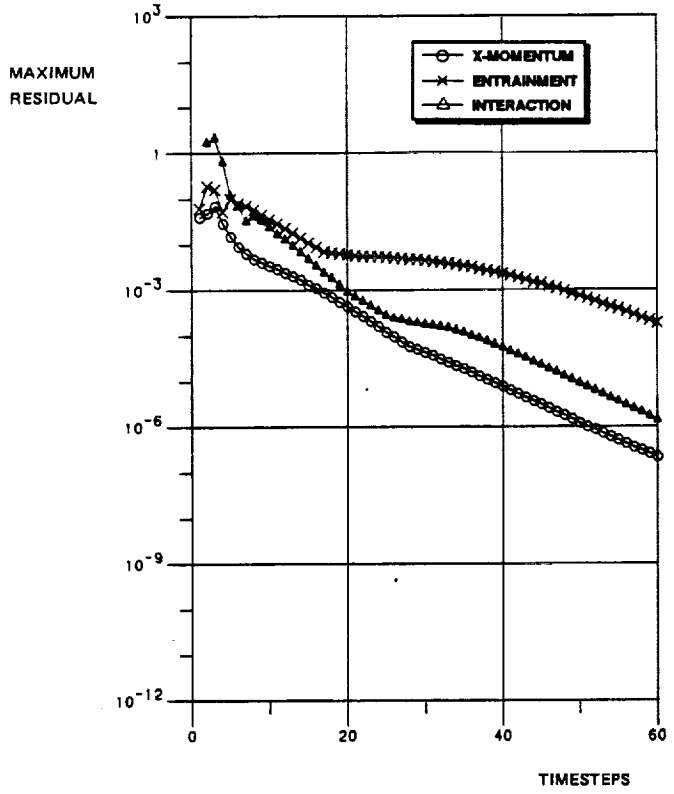


a) Maximum residual vs. timesteps
$M_\infty = 0.70$, $\alpha = 0$, $Re = 9 * 10^6$

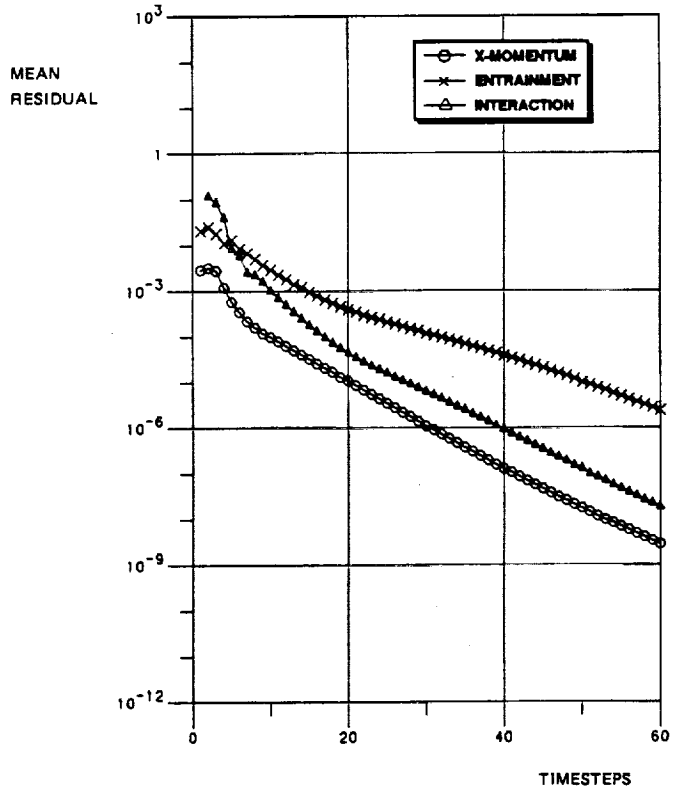


b) Mean residual vs. timesteps
$M_\infty = 0.70$, $\alpha = 0$, $Re = 9 * 10^6$

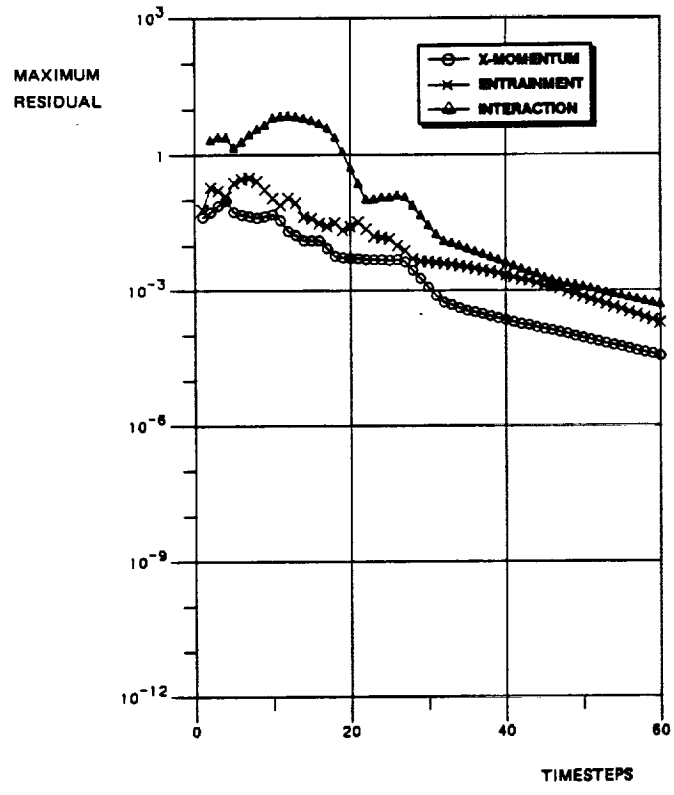


c) Maximum residual vs. timesteps
$M_\infty = 0.799$, $\alpha = 2.26$, $Re = 9 * 10^6$

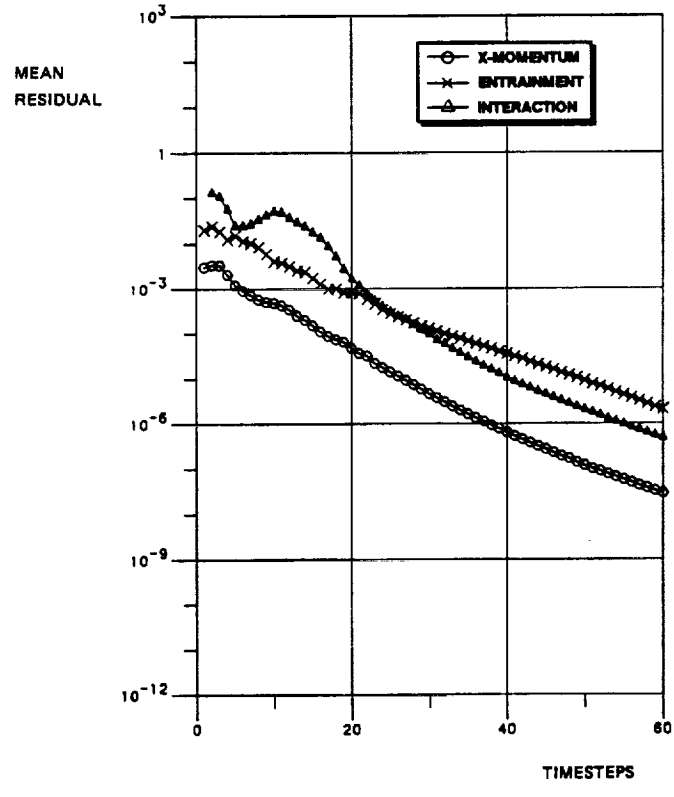


d) Mean residual vs. timesteps
$M_\infty = 0.799$, $\alpha = 2.26$, $Re = 9 * 10^6$

Fig. 3 Convergence histories for boundary layer computation on a NACA-0012 straight wing

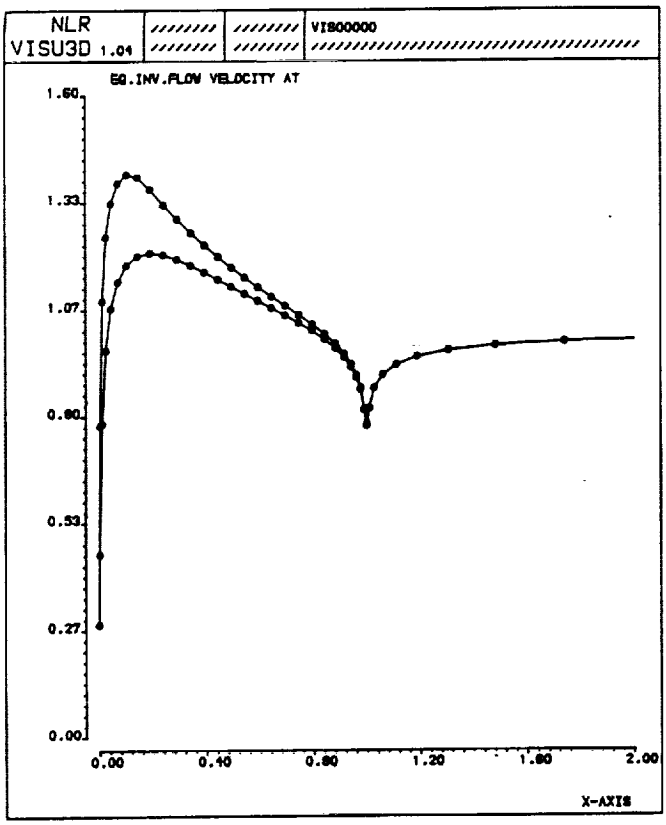


a) Inviscid flow velocity distribution

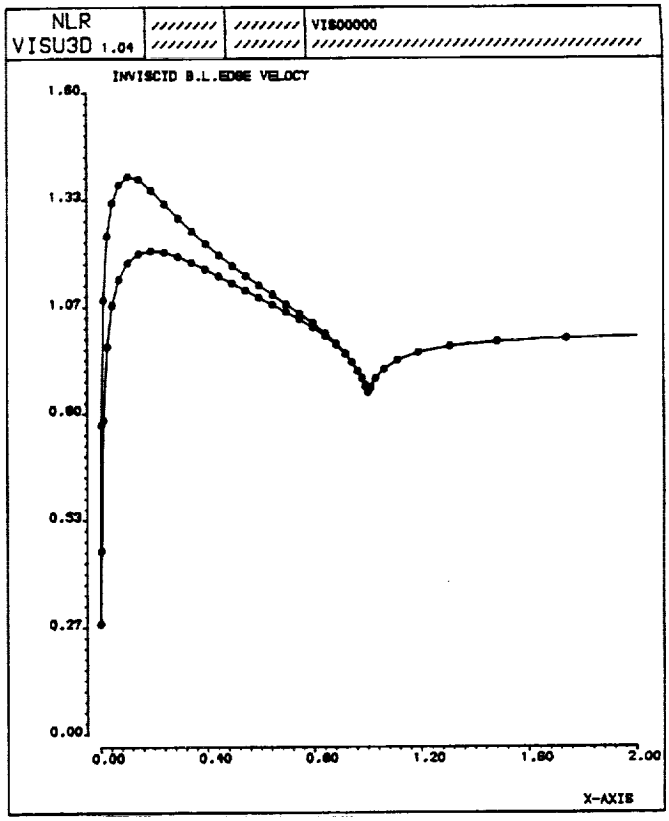


b) Viscous flow velocity distribution

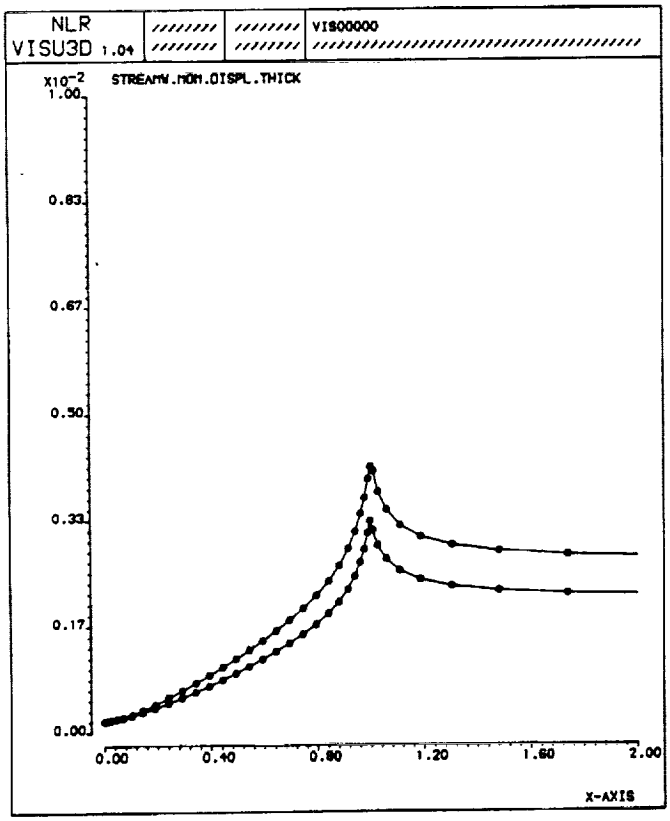


c) Boundary layer streamwise momentum thickness

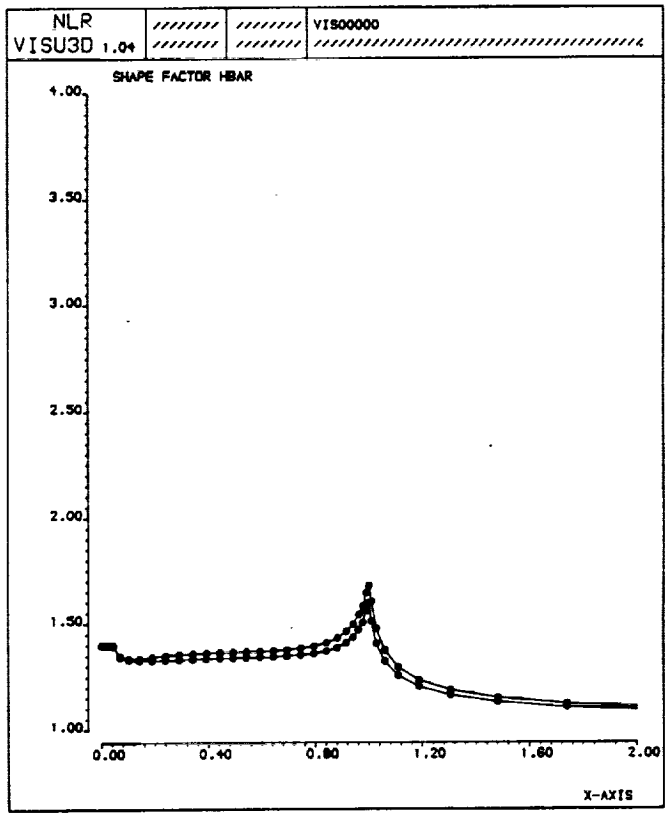


d) Boundary layer shape factor $\overline{H}$

Fig. 4 Viscous-inviscid interaction results for root section of a NACA-0012 straight wing at $M_\infty = 0.70$, $\alpha = 1.49$, $Re = 9 * 10^6$

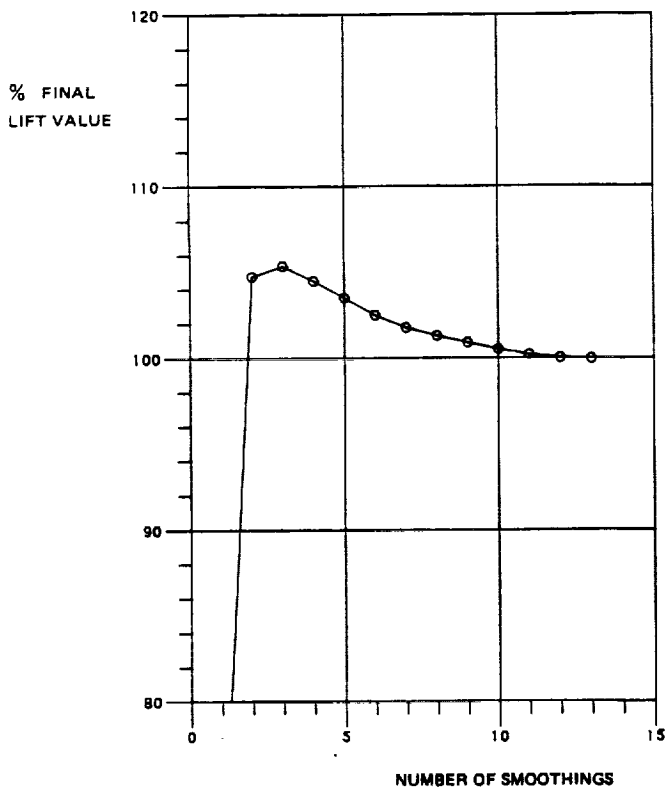


a) Lift coefficient of wing

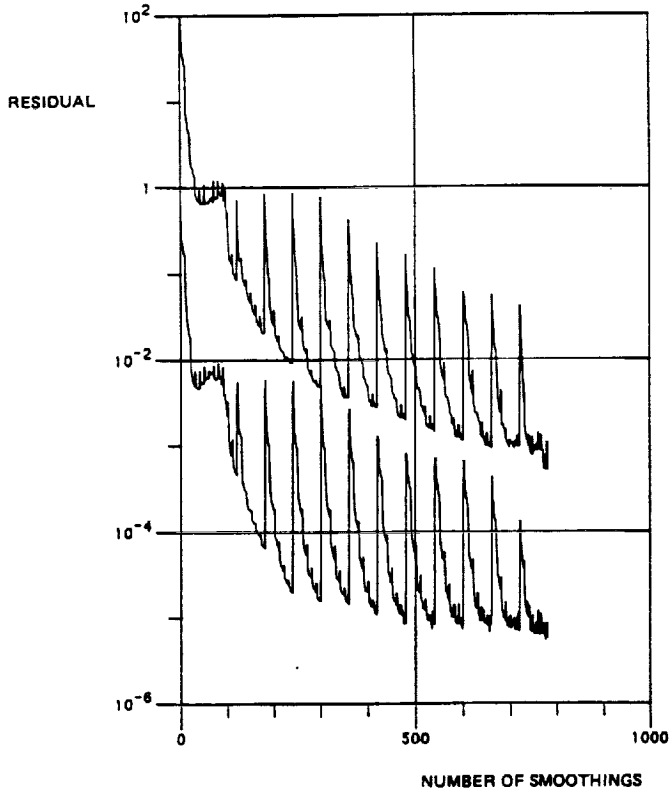


b) Maximum and mean residual

Fig. 5 Convergence histories for viscous-inviscid interaction computation on a NACA-0012 straight wing at $M_\infty = 0.70$, $\alpha = 1.49$, $Re = 9\ 10^6$

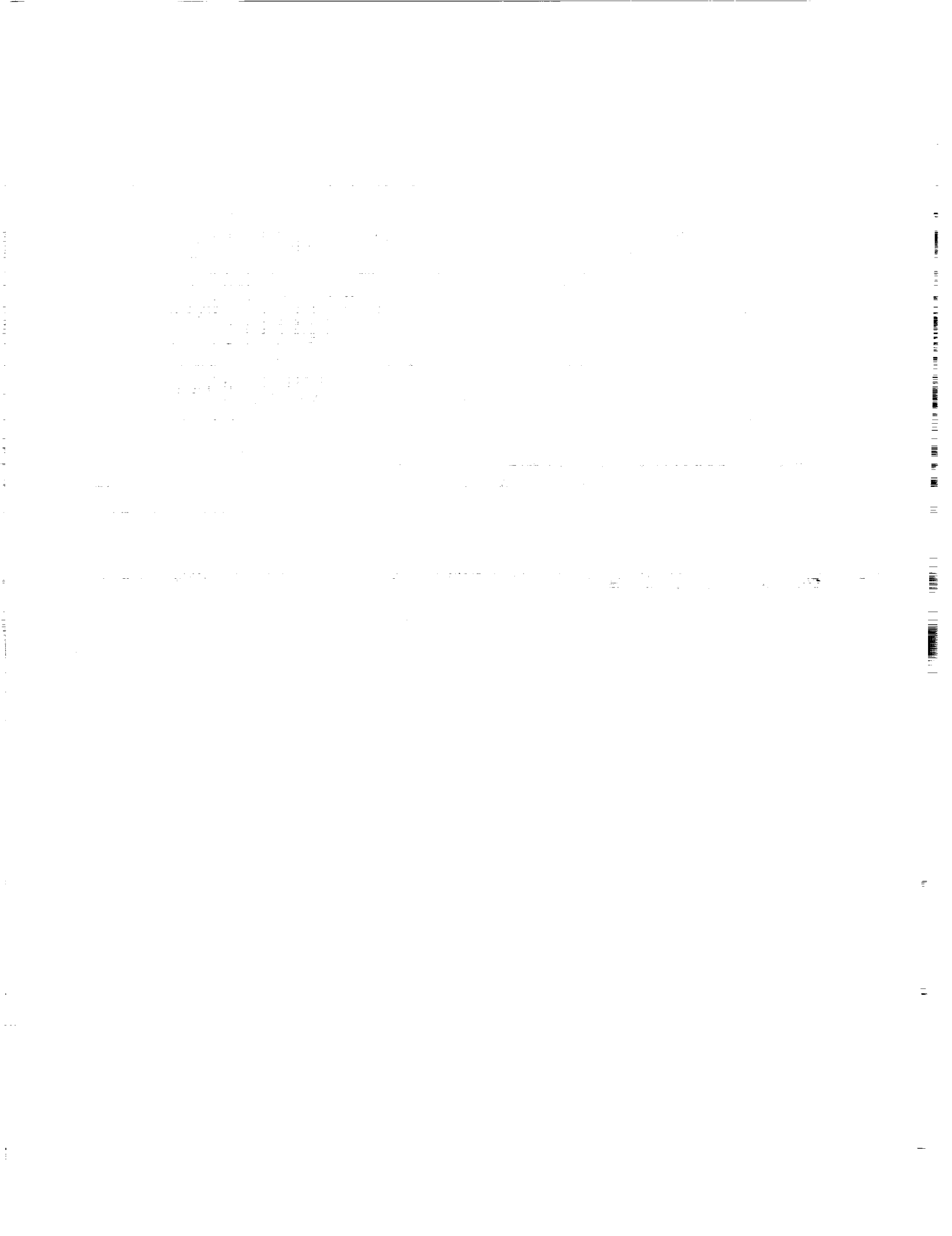

# TWO- AND THREE-DIMENSIONAL FLOWS, 4
# SESSION 12